A Multivariate Approach for Drowsiness Detection Using Empirical Fourier Decomposition

Ashok Mahato, Kritiprasanna Das, and Ram Bilas Pachori, *Senior Member, IEEE*

***Abstract*—In this study, our goal is to investigate the multivariate rhythmic characteristics of electroencephalogram (EEG) and electrooculogram (EOG) data in adaptive frequency scales for drowsiness detection. The empirical Fourier decomposition (EFD) method has been extended to multivariate signals to eliminate the mode alignment issue in multichannel signals. The proposed multivariate EFD (MEFD) is designed to adapt mode alignment to extract mutual characteristics across multi-channel and delivered channel-aligned modes. This novel technique utilizing an adaptive zero-phase filter bank, optimized boundary estimation, and a MEFD-based multi-model framework has been introduced to enhance drowsiness recognition performance by addressing invariant sampling rates across EEG and EOG modalities. In order to test effectiveness, the proposed MEFD has been investigated using multichannel synthetic signals, and EEG and EOG signals from the SEED-VI drowsiness database. Further feature fusion matrix (FFM) has been formed to extract mutual information from multivariate multimodal EEG and EOG signals. Finally, the obtained FFM features have been tested using six well-known classifiers. With 5-fold cross-validation, our proposed MEFD-based classification framework has demonstrated exceptional performance in drowsiness state classification, achieving the highest accuracy of 82.3% when compared to state-of-the-art methods.**

***Index Terms*—Multivariate empirical Fourier decomposition, Multivariate signal, drowsiness detection, Electroencephalography, Electrooculography.**

I. Introduction

Detecting drowsiness is crucial, as it significantly reduces the risk of accidents caused by a driver's instant loss of focus while driving. Drowsiness is a condition that occurs intermittently between states of being completely alert and completely fatigued [1]. It can be caused by several different factors, including working long hours, taking medicine, not getting enough sleep, or driving for an extended period of time. It makes a person less focused and vigilant toward the activities that person is currently carrying out. This issue could be resolved with the implementation of a drowsiness detection and early warning system [1]. Eye closing, eye blinking, and head posture are taken into consideration by the behavioural measure to identify a sleepy condition.

Ashok Mahato is with the Department of Electrical Engineering, Indian Institute of Technology Indore, Indore-453552, India (e-mail: phd2101102003@iiti.ac.in).

Kritiprasanna Das is with the Department of Electrical Engineering, Indian Institute of Technology Indore, Indore-453552, India (e-mail: phd1901102016@iiti.ac.in).

Ram Bilas Pachori is with the Department of Electrical Engineering, Indian Institute of Technology Indore, Indore-453552, India (e-mail: pachori@iiti.ac.in).

Biological signals such as the electroencephalography (EEG) [2], electrooculography (EOG) [3], electrocardiography (ECG) [4], and electromyography (EMG) [3] are used in the detection drowsiness. An ECG, on the other hand, is primarily used to monitor cardiac activity and may not accurately represent changes in cognition linked to sleepiness. Muscle activity is measured by EMG, which is less specific for detecting sleepiness early on and might not record the required neurological and cognitive signals, making them less ideal for this particular application. Due to their direct correlation with the neurological and cognitive components of alertness, EEG and EOG are the preferred methods for detecting drowsiness [2], [5]. Because EEG is so sensitive to mental state changes and measures electrical brain activity, it is the best tool for identifying changes in brain activity associated with drowsiness, such as theta and delta waves [1]. EOG captures eye movements and blink patterns, offering information on microsleeps and eye fatigue—common symptoms of sleepiness [6]. By combining these signals, one can obtain a comprehensive understanding of the physiological changes that occur during drowsiness, which facilitates the early detection of subtle shifts between alertness and drowsiness.

In recent many, drowsiness detection through EEG signals has been explored with a number of different approaches. The moving average power spectrum analysis and principal component analysis (PCA) were combined to extract the feature matrix's from EEG signals [7]. These features were then used to train fuzzy neural networks to detect drowsiness. In [8], independent component analysis (ICA), fast Fourier transform (FFT), correlation assessment, and a linear regression model were used to design a drowsiness-detection framework. The ICA-based approach can eliminate most of the EEG artifacts from the FFT spectrum of the ICA component. In another study [9], authors have applied FFT to the data before using a bandpass filter to obtain the intended frequency EEG rhythms. The authors claim that only alpha and beta rhythms are helpful for drowsiness detection. In [10], authors segmented the signal from an EEG channel, extracted power-related features using FFT, and fed these features to an artificial neural network (ANN) and support vector machine (SVM) for classification. In another work [11], the short-time Fourier transform (STFT) was used to calculate the average relative power features for alpha and beta rhythms and then these features were passed through a mean comparison test to detect drowsiness. In [12]- [13], the wavelet transform-based method is used for automated drowsiness detection due to its multi-resolution capability to measure EEG energy at each decomposition level. In another study [14], authors presented

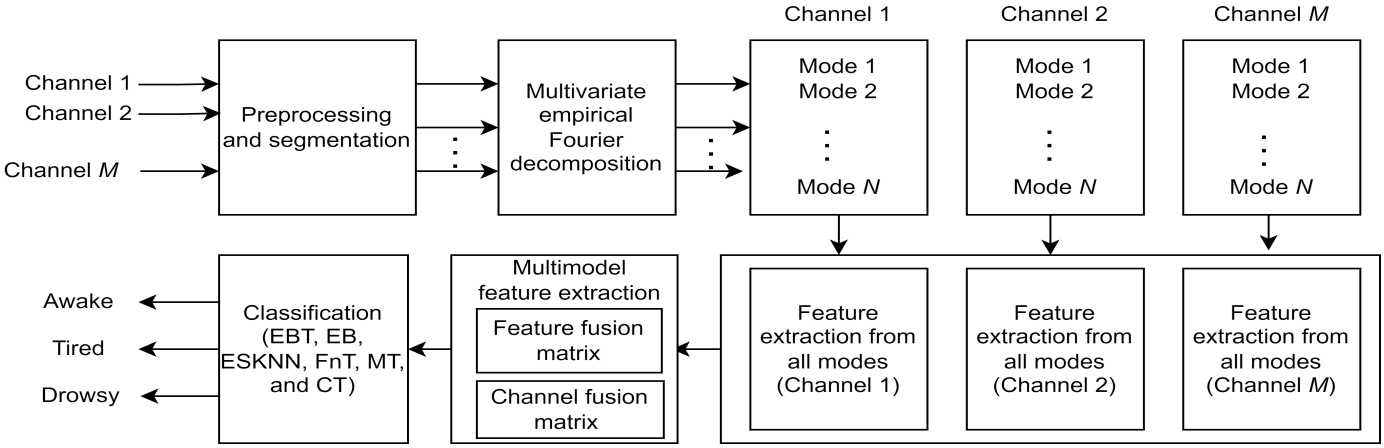

Fig. 1. Block diagram of proposed MEFD-based drowsiness detection framework.

a method for detecting sleepiness that involves using the best m-term estimate on single-channel EEG data that has been processed using a discrete wavelet transform. In [15], the normalized Haar discrete wavelet packet transform (WPT) is used to calculate spectral power-based characteristics from EEG rhythms to detect drowsiness. The Haar WPT enables specific resolution of brain rhythms into packets and requires only a small amount of processing work. In the multimodal analysis approach [16], time series, frequency spectrum, and wavelet decomposition were used to differentiate between activeness and drowsiness. Features were calculated from single-channel EEG, and afterwards, feature selection was performed based on lambda of Wilks criterion. The selected features are fed as input to ANN classifier. In [17], intrinsic mode functions from empirical mode decomposition (EMD) were used to separate EEG rhythms, and the Hilbert transform was used to calculate the instantaneous frequency of each rhythm [18]. To classify drowsiness, time domain features from distinct EEG rhythms were computed and analyzed using different ensemble classifier variations. In another approach, various deep learning models, such as recurrent neural networks [19], long short-term memory networks [20], and convolutional neural networks (CNNs) [21], [22] have found application in the field of drowsiness detection. Among these models, CNNs are predominantly favored for drowsiness detection tasks owing to their exceptional classification performance.

Every approach has its own advantages and disadvantages. FFT-based transform converts the time domain signal into the frequency domain, but the time localization is absent as opposed to the time-frequency domain. STFT still has a problem in choosing windows and their lengths. Decomposition with wavelet-based methods requires choosing the wavelet and the number of levels manually. The choice of filter coefficients remains tough when using filtering methods. There is no mathematical modeling in the EMD-based approach, which is strictly experimental and suffers from mode-mixing. In comparison to a traditional machine learning algorithm, CNN is more costly, requires more data, and takes longer to train. For these reasons, CNN-based models are not recommended for drowsiness monitoring.

Therefore our research, we have introduced a drowsiness detection strategy based on novel multivariate empirical Fourier decomposition (MEFD). With MEFD, signals are separated adaptively into the appropriate number of modes, and extracts the entropy, time series, and statistical-based characteristics of each mode to construct a feature vector. Then feature space can be used for classification into awake, tired, and drowsy states using a machine learning classifier. The MEFD-based classification model is illustrated in Fig. 1. We have a multimodal framework for drowsiness detection from EEG and EOG signals. Additionally, we have introduced channel fusion and feature fusion matrix within this multimodal framework to enhance drowsiness detection based on EEG and EOG signals. For multimodality, we discovered that channel fusion shows better performance than feature fusion. It proves the usefulness and efficiency of our method.

The remaining sections of the paper are organized in the following way. In the second section of this study, we will discuss the data set that is utilized in this investigation. An explanation of the methods can be found in section 3. Section 4 presents the results and discussions. The last section concluded the proposed work.

II. Dataset Description

In this study, we used SEED-VIG dataset, which is openly available [6]. This data set is collected using a virtual-reality simulation driving system. There are 23 subjects in the SEED-VIG dataset (11 males and 12 females; average age: 23.3 years). Using the Neuroscan device with a 1000 Hz sample rate, the EOG and EEG signals were captured simultaneously for 118 minutes. An international 10–20 electrode system was used to record 12-channel EEG signals from the posterior site (CP1, CPZ, CP2, P1, PZ, P2, PO3, POZ, PO4, O1, OZ, and O2), 6-channel signals from the temporal site (FT7, FT8, T7, T8, TP7, and TP8), and 7-channel have been used to capture EOG signals. Percentage of eye closure (PERCLOS) level are used in this dataset for awake, tired and drowsiness states [6]. In order to determine PERCLOS, the eye closure time is measured in every $8S$ with the help of eye tracking glass. We divided the level values into three categories awake, tired,

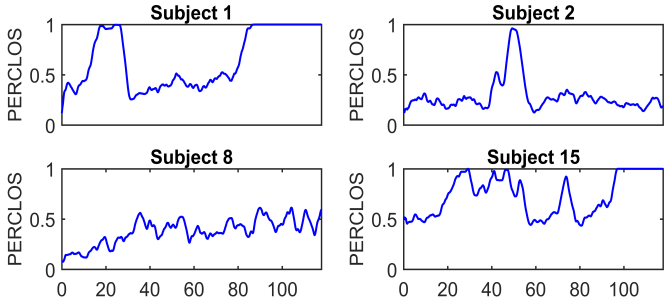

Fig. 2. Epoch-wise PERCLOS level for four randomly selected subjects.

TABLE I
SUBJECT-WISE NUMBER OF EPOCHS IN EACH CLASS

Subject number	Class			Subject number	Class		
	Awake	Tired	Drowsy		Awake	Tired	Drowsy
1	114	387	384	13	324	545	16
2	767	72	46	14	321	86	478
3	93	709	83	15	0	407	478
4	503	323	59	16	225	464	196
5	258	401	226	17	289	525	71
6	458	178	249	18	202	177	506
7	422	304	159	19	26	710	149
8	313	572	0	20	424	109	352
9	98	753	34	21	145	723	17
10	701	87	97	22	625	50	210
11	208	636	41	23	616	107	162
12	273	576	36				

and drowsy by using two thresholds (0.35 and 0.7) for the classification. The PERCLOS level of different subjects as shown in Fig. 2. Table I provides a summary of each subject's epoch distribution over the three classes (awake, tired, and drowsy). Although our dataset initially includes data from 23 subjects, some imbalances in the data, as outlined in Table I, lead us to exclude specific subjects (8, 12, 13, 15, and 21). Notably, as per Table I, subjects 8 and 15 present data with only two available classes.

III. METHODOLOGY

This methodology consists of decomposing the signal into modes using MEFD grouping to obtain EEG rhythms, selection of features, and classifying the patterns to detect drowsiness. In Fig. 1, block diagram is briefly illustrated in the following subsections.

A. Data Preprocessing and Segmentation

The raw EEG and EOG signals are preprocessed using a band-pass filter having cut-off frequencies 1 Hz and 75 Hz to remove artifacts and noise. The signals are downsampled (200 Hz for EEG, 125 Hz for EOG) to decrease computational complexity. The 118 min of EEG and EOG data are segmented for each individual using 8 *sec* time frame, which resulted in a total of 885 segments. It is important to highlight that each sample in this investigation is a two-dimensional matrix, with 1600 data points coming from 17 channels for EEG data (1600 $\times$ 17) and 1000 data points coming from 7 channels for EOG (1000 $\times$ 17) data.

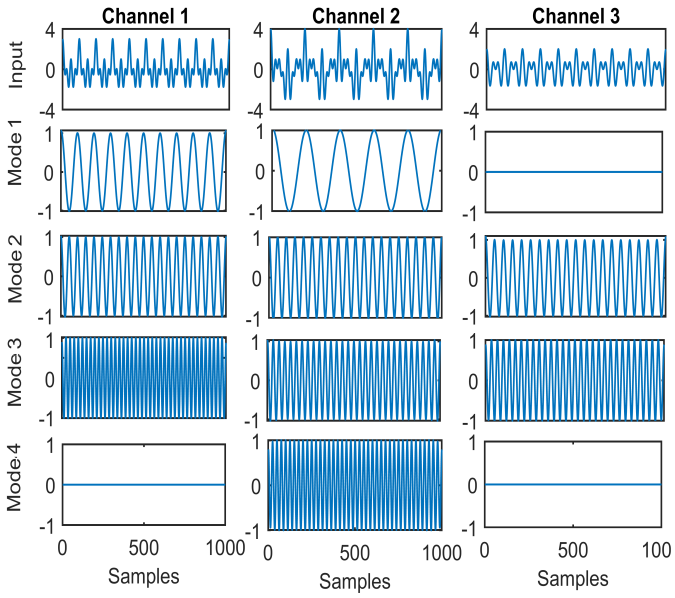

Fig. 3. Multivariate analysis using existing EFD method across N-channel represent the mode-alignment issue.

B. Multivariate Empirical Fourier Decomposition

The proposed MEFD is an extension of the EFD method [23] to enhance multivariate signal analysis to eliminate the mode alignment issue in multichannel signals and enhance channel-aligned mode across channels [24]. In MEFD, it adopts an improved filter bank and optimal boundary selection to enhance signal characteristics across channels with noise reduction; thus, it enhances drowsiness recognition. EFD uses an adaptive and univariate approach to decompose single-channel signals into channel-specific modes which do not exhibit mutual characteristics among the multivariate multichannel data. It creates mode-alignment problems for multivariate analysis, which is demonstrated in Fig. 3. From the multivariate analysis mentioned in Fig. 3, it is observed that the obtained modes across channels do not show similar characteristics. For example, extracted similar mode 2 is present in all channels which exhibit mutual information, whereas mode 1 and mode 4 are present in channel-specific with channel 1 and channel 2.

The MEFD involves three important processes: Mean spectrum computation, an enhanced spectrum segmentation method (ESM), and the designing of a zero-phase filter bank (ZFB).

1) Mean spectrum estimation for multivariate analysis: Let us consider that the multivariate time series data $s(t)$ which can be expressed as follows:

$$s(t) = \begin{bmatrix} s_1(t) \\ s_2(t) \\ \vdots \\ s_M(t) \end{bmatrix} \tag{1}$$

where M is the number of channels. In order to align multivariate multichannel signal across channels, we have adopted

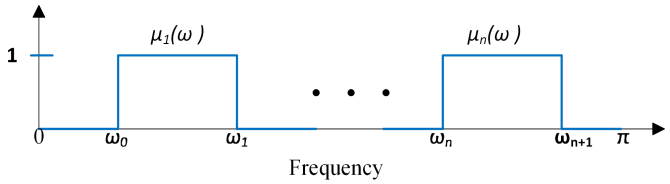

Fig. 4. Ideal filter bank response of the EFD.

the mean spectrum magnitude to find common boundaries across channels. The computed mean spectrum from multi-channel signals $s(t)$. It is computed as follows:

$$S(f) = \frac{1}{M} \sum_{m=1}^{M} |S_m(f)| \tag{2}$$

where $S_m(f)$ is the Fourier spectrum of channel m. The range of the parameter m is 1 to M.

2) Enhanced spectrum segmentation method: The enhanced segmentation method (ESM) is based on the lowest minima approach [25]. In this method, $[0, \pi]$ can be divided into N distinct frequencies. In contrast to the conventional methods of identifying local maxima and lowest minima, the values of ω_0 and ω_N in this approach are not fixed at 0 and π, respectively. Instead, it is determined through an adaptive sorting process. During the sorting procedure, the Fourier spectrum magnitudes at ω = 0 and ω = π, along with their respective local maxima, are determined out and gathered into a sequence. Subsequently, all magnitudes within this sequence are arranged in descending order. [Ω_1, Ω_2, ..., Ω_N] denotes frequencies corresponding to the first N largest values in the sorted order. Additionally Ω_0 is defined as 0 and Ω_{N+1} is defined as π. Finally, the boundaries ω_n of each segment can determined by,

$$\omega_n = \begin{cases} \underset{\omega}{\operatorname{argmin}} \left(S_n(\omega)\right), & \text{if } 0 \leq n \leq N \text{ and } \Omega_n \neq \Omega_{n+1} \\ \Omega_n, & \text{if } 0 \leq n \leq N \text{ and } \Omega_n = \Omega_{n+1} \end{cases} \tag{3}$$

where $S_n(\omega)$ represents the magnitude of the Fourier spectrum between order range Ω_n and Ω_{n+1}.

3) Designing of a modified zero-phase filter bank: A zero-phase filter is a band-pass filter that operates in each frequency band, and it has no transition band with cut-off frequencies between ω_{n-1} and ω_n which were obtained from ESM. As a result, the zero-phase filter can keep the most important component of the Fourier spectrum that is contained inside the segment, while excluding any other Fourier spectrum components that extend beyond the segment.
Fourier transform (FT) is used to obtain spectrum $\hat{s}(\omega)$ from signal $s(t)$. Then, a zero-phase filter bank $\mu_n(\omega)$ is constructed as,

$$\mu_n(\omega) = \begin{cases} 1, & \text{if } \omega_{n-1} \leq |\omega| \leq \omega_n \\ 0, & \text{otherwise} \end{cases} \tag{4}$$

Where $1 \leq n \leq N$ and values of ω_n are determined by Eq 3. Figure 4 shows a graphical representation designing of ZFB.

The filtered signal $\hat{s_n}(\omega)$ corresponds to $\mu_n(\omega)$ is calculated using following equation:

$$\hat{s_n}(\omega) = \mu_n(\omega)\hat{s}(\omega) = \begin{cases} \hat{s}(\omega), & \text{if } \omega_{n-1} \leq |\omega| \leq \omega_n \\ 0, & \text{otherwise} \end{cases} \tag{5}$$

The decomposed component $s_n(t)$ in the time domain can be constructed using inverse FT of $\hat{s_n}(\omega)$. Reconstructed signal $\tilde{s}(t)$ is calculated as the sum of all components of the decomposed signal, which is defined as follows:

$$\tilde{s}(t) = \sum_{n=1}^{N} s_n(t) \tag{6}$$

We can locate the boundaries of $S(f)$ using the ESM, and filter this signal using a ZFB. The next step is to decompose each channel using the generated filter bank. In this case, the number of modes generated for each channel will be the same, and the frequency support of each channel's modes will be the same for all oscillation levels, which is shown in Fig. 5. This method can also be tested for noisy signals and as well as some non-stationary multichannel and modulated signals.

The multivariate signal representation can be presented as follows after the decomposition of the multivariate signal $s(t)$, which is given as follows:

$$s(t) = \begin{bmatrix} s_{11}(t) & s_{12}(t) & \dots & s_{1N}(t) \\ s_{21}(t) & s_{22}(t) & \dots & s_{2N}(t) \\ \vdots & \vdots & \ddots & \vdots \\ s_{M1}(t) & s_{M2}(t) & \dots & s_{MN}(t) \end{bmatrix} \tag{7}$$

where N is the number of decomposed modes. The range of the variable n is 1 to N. The procedure of the MEFD method can be outlined as Algorithm 1.

Algorithm 1 MEFD algorithm

Require: Multivariate signal $s(t) \in \mathbb{R}^{M \times L}$, where M is the number of channel L is the length of the signal.
Ensure: Extraction of modes $\tilde{s}(t) \in \mathbb{R}^{M \times N \times L}$, where N is the number of modes.
1: Obtain the spectrum for all channels of the input signal using FT.
2: Compute the mean spectrum magnitudes $S(f)$ from all channels.
3: Determine the local maximum and minimum values of the spectrum.
4: Sort the frequencies corresponding to the largest values of the spectrum in ascending order for each channel.
5: Detect the boundaries of the signal using the lowest minima technique for each channel.
6: Construct and filtered the signal using a zero-phase filter bank.
7: Convert the filtered signal into a time domain signal $\tilde{s}(t)$ using an inverse FT.

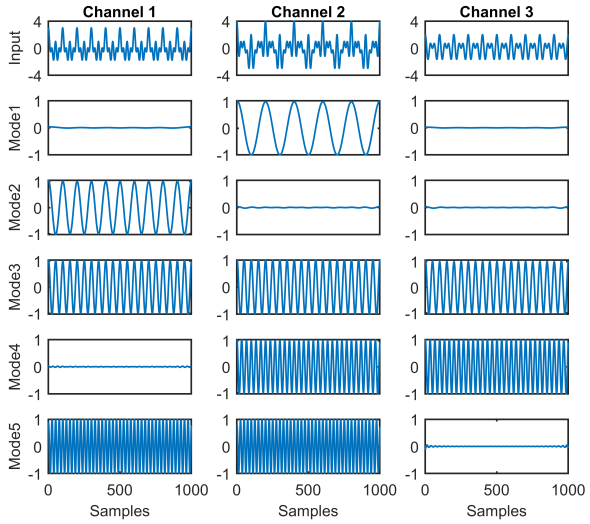

Fig. 5. Time-domain representations of the multi-channel signal and its obtained subbands.

4) Validation of proposed MEFD on multivariate synthetic signal and real EEG signal: In order to demonstrate the performance of the proposed MEFD, we have used synthetic multivariate multi-component signal $z(t)$, which is represented as follows:

$$z(t) = \begin{bmatrix} z_1(t) \\ z_2(t) \\ z_3(t) \end{bmatrix} \tag{8}$$

where
$z_1(t) = \cos(20\pi t) + \cos(40\pi t) + \cos(80\pi t)$
$z_2(t) = \cos(10\pi t) + \cos(40\pi t) + \cos(60\pi t) + \cos(80\pi t)$
$z_3(t) = \cos(40\pi t) + \cos(60\pi t)$

we have employed a multivariate time series signal with a sampling frequency 1 kHz. Fig. 5 shows that the MEFD method produces properly matched modes in each of the three channels for synthetic signals. The proposed method can also be applied to a given EEG dataset. Fig. 6 shows that each mode across multiple channels and properly aligns them for real EEG signals.

C. Feature Extraction

There are several EEG features that have been reported in the literature for detecting drowsiness [5]. To identify an optimal feature set across cross-modalities i.e. EEG and EOG, we have employed time and frequency domain features, which show significant improvement related to multi-class drowsiness recognition. Further, to find discriminative features, we have presented a multi-model fusion approach based on channel fusion matrix (CFM) and feature fusion matrix (FFM). Table II shows the 18 different features, descriptions, and formulas used in our study. The selection of these features is due to their significant performance mentioned in earlier research work [5].

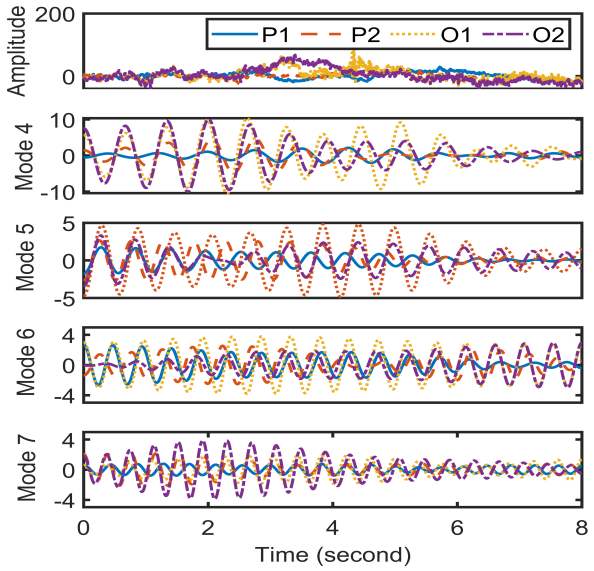

Fig. 6. Decomposition of 4-channel EEG signals and its selected channel-aligned modes.

D. Classification

Six machine learning classifiers were used in our study: ensemble boost (EBT), ensemble bagged (EB), ensemble subspace KNN (ESKNN), fine tree (FnT), medium tree (MT), and coarse tree (CT) [28]. EBT is a method for machine learning that trains weak models one by one, with each new model working on fixing the errors of the previous ones. The predicted result of the boosted decision tree classification for a new input feature vector x is denoted as $H(x)$ and is given by the following equation:

$$H(x) = \text{sign}\left(\sum_{m=1}^{M} \alpha_t h_t(x)\right) \tag{9}$$

The EB tree creates a collection of decision trees through the bagging process, with each tree being trained using a different subset of the training data. This ensemble classifier's prediction result is obtained using the following equation and represented as $H(x)$:

$$H(x) = \text{sign}\left(\sum_{m=1}^{M} h_t(x)\right) \tag{10}$$

where M is the number of decision trees and $h_t(x)$ is the output of the m^{th} weak classifier for input x and α_t is the weight assigned to the m^{th} weak classifier.

In the case of ESKNN classifier [28], we are combining multiple KNN classifiers which are trained on different feature subsets. The mathematical representation is given as,

$$H(x) = \text{mode}(K_1(x), K_2(x)...K_M(x)) \tag{11}$$

The decision tree is a logic-based method where datasets can be model in hierarchical structures by comparing a sequence of if-else statements. Depending on the maximum number of splits, it can be categorized into three groups, which are FnT,

TABLE II
LIST OF FEATURES USED IN OUR WORK.

Feature number	Feature	Measuring parameters	Formula
1	Mean	It is a statistical feature used to measure the average value of a set of data points in a signal.	$\mu = \frac{1}{N}\sum_{n=1}^{N} x_n$
2	Standard deviation	It quantify the variability of a set of data points in a signal.	$\sigma = \sqrt{\frac{\sum_{n=1}^{N}(x_n-\mu)^2}{N}}$
3	Variance	It measures the spread of data points within a signal.	var $= \sigma^2$
4	Median	It describe the central tendency of a set of data points in a signal.	med $=$ med$[X_n]$
5	Maximum	It represents the highest value within a set of data points in a signal.	max $=$ max$[X_n]$
6	Minimum	It represents the lowest value within a set of data points in a signal.	min $=$ min$[X_n]$
7	Kurtosis	It measures the concentration of data points in the tails of a distribution.	KS $=$ kurtosis$[X_n]$
8	Skewness	It measures the asymmetry of the probability distribution of a signal.	SN $=$ skewness$[X_n]$
9	Hjorth activity [26]	It provides a measure of the overall energy of the signal.	HA $= \sigma_0^2$
10	Hjorth mobility [26]	It characterizes how rapidly the signal changes over time.	HM $= \frac{\sigma(x^{'}(n))}{\sigma(x(n))}$
11	Hjorth complexity [26]	It provides insights into the variations and changes in the signal's waveform over time.	HC $= \frac{\text{HM}(x^{'}(n))}{\text{HM}(x(n))}$
12	Mean energy [27]	The mean energy represents the total amount of energy over a given period.	ME $= \frac{1}{N}\sum_{n=k-N+1}^{k} x[n]^2$
13	Mean teager energy [27]	It's capturing the changes in energy over time.	$MTE = \frac{1}{N}\sum_{n=k-N+3}^{k}(x[n-1]^2 - x[n]x[n-2])$
14	Shannon entropy [5]	It determines how much knowledge is needed to separate random samples from signal.	SE $= -\sum_{n=1}^{N} p(x_n)\ \log\ p(x_n)$
15	Tsallis entropy [5]	It measures the degree of uncertainty or randomness in a signal's probability distribution.	TE $= \frac{1-\sum_{n=1}^{N} p(x_n)^q}{q-1}$
16	Renyi entropy [5]	It provides a measure of the diversity of information in a signal.	RE $= \frac{1}{1-b}(\log\ \sum_{n=1}^{N} p(x_n)^b)$
17	Log energy entropy [5]	It measures the complexity of signals.	LEE $= -\sum_{n=0}^{N-1} \log_2\ (p(x_n))^2$
18	Differential entropy [5]	It measure the information content per unit interval in a continuous distribution.	$H(X) = -\int f(x)\ \log\ f(x)\ dx$

μ is the mean of the signal, N represents total number of samples of the signal, x_n is the value of the n^{th} sample of signal, σ and σ^2 are standard deviation and variance of the signal. X_n represents time series signal. $p(x_n)$ represent the probability of the n^{th} outcome of the time series signal X. q is the Tsallis entropy parameter, it is calculated for $q = 2$ ($q \neq 1$ and $q > 0$). b is the order parameter.

MT and CT. Table III compares different types of classifiers based on their parameter settings and shows how they differ in terms of complexity, performance, and accuracy.

IV. RESULTS AND DISCUSSION

In order to test the effectiveness of the proposed MEFD-based drowsiness recognition, we have tested on real-time EEG SEED-VI drowsiness dataset [6]. To assess the performance MEFD-based classification framework across all three classes (Awake, Drowsy, and Tired), we have used four performance measures [34], [35]: Accuracy ($Acc = \frac{(TP+TN)}{(TP+TN+FP+FN)}$), sensitivity ($Sen = \frac{(TP)}{(TP+FN)}$), specificity ($Spe = \frac{(TN)}{(TN+FP)}$), and F1-score ($F1 = \frac{(TP+TN)}{(TP+TN+FP+FN)}$). Here, TP (true positives), FP (false positives), TN (true negatives), and FN (false negatives) play vital roles in defining these metrics. In the experimentation, we have conducted two fusion feature multi-models: Model 1 and model 2. Model 1 integrates channel fusion across multi-channel EEG and EOG signals, while Model 2 incorporates the fusion of 18 features computed from various combinations. In the training-testing process, we have configured six different machine learning classifiers (EBT, EB, ESKNN, FnT, CT, and

TABLE III
SET OF PARAMETERS USED IN DIFFERENT ML CLASSIFIERS.

Classifier	Parameters	Values
Ensemble boosted tree	Ensemble method	AdaBoost
	Learner type	Decision tree
	Maximum number of splits	20
	Number of learner	30
	Learning rate	0.1
Ensemble bagged tree	Preset	Bagged tree
	Ensemble method	Bag
	Learner type	Decision tree
	Maximum no. of splits	884
	Number of learner	30
Ensemble subspace KNN	Preset	KNN
	Ensemble method	Subspace
	Learner type	Nearest neighbors
	Number of learner	30
	Subspace dimension	1530
Fine tree	Preset	Fine tree
	Maximum number splits	100
	Split criterion	Gini's diversity index.
Medium tree	Preset	Medium tree
	Maximum number splits	20
	Split criterion	Gini's diversity index.
Coarse tree	Preset	Coarse tree
	Maximum number splits	4
	Split criterion	Gini's diversity index.

TABLE IV
EVALUATED CLASSIFICATION PERFORMANCE PARAMETERS WITH FIVE-FOLD CROSS VALIDATION USING DIFFERENT CLASSIFIERS FOR EEG

Sb	Ensemble boosted				Ensemble bagged				Ensemble subspace KNN				Fine tree				Medium tree				Coarse tree			
	Acc	Spe	Sen	F1	Acc	Spe	Sen	F1	Acc	Spe	Sen	F1	Acc	Spe	Sen	F1	Acc	Spe	Sen	F1	Acc	Spe	Sen	F1
1	83.8	91.1	74.8	0.76	84.2	91.4	74.5	0.76	77.0	87.3	67.0	0.68	76.7	87.6	69.0	0.69	79.4	89.1	71.5	0.72	82.0	91.0	76.3	0.76
2	88.4	71.9	46.7	0.51	87.0	68.8	48.7	0.40	85.2	76.0	54.4	0.56	77.8	72.0	45.3	0.45	79.4	72.3	44.5	0.45	85.7	70.7	42.4	0.45
3	88.4	83.4	69.2	0.74	87.0	81.0	63.0	0.66	80.1	75.3	52.0	0.55	80.4	81.2	65.3	0.65	82.2	80.0	62.4	0.64	85.0	79.3	61.0	0.65
4	69.7	80.2	50.4	0.51	71.0	80.0	50.0	0.49	62.1	76.5	52.0	0.52	60.0	75.7	47.0	0.47	65.6	78.5	48.5	0.49	64.3	77.1	47.1	0.48
5	60.4	78.3	59.0	0.39	62.0	80.0	62.0	0.62	48.0	73.0	47.0	0.47	52.0	74.5	51.2	0.51	57.2	77.0	55.3	0.56	56.1	76.0	54.1	0.55
6	72.1	83.6	60.1	0.46	74.2	84.5	62.3	0.60	70.0	83.5	63.0	0.62	61.7	80.1	55.5	0.55	72.0	84.3	63.0	0.62	71.0	83.0	58.4	0.53
7	78.6	88.6	77.6	0.78	78.0	88.0	77.0	0.78	68.3	83.0	67.4	0.68	69.0	83.4	68.1	0.68	72.7	85.3	72.1	0.73	69.3	84.1	67.0	0.67
9	89.7	80.1	71.1	0.74	88.3	81.0	71.0	0.72	85.0	76.3	62.2	0.64	82.3	79.1	68.0	0.67	84.5	77.2	63.0	0.65	88.0	81.0	71.0	0.72
10	88.3	87.0	64.4	0.63	89.0	87.0	65.0	0.64	88.6	90.0	72.8	0.72	83.0	86.7	63.2	0.63	84.0	86.0	63.0	0.63	87.3	87.0	63.0	0.62
11	73.2	70.6	48.5	0.49	70.0	68.0	40.0	0.41	63.7	71.5	49.3	0.49	59.0	69.0	48.6	0.46	66.0	70.5	44.4	0.46	69.0	68.0	44.1	0.43
14	87.9	92.5	67.8	0.67	87.0	92.2	66.0	0.65	78.7	88.0	61.0	0.61	74.5	87.4	59.2	0.60	80.7	90.0	63.0	0.63	84.8	91.4	65.1	0.65
16	58.8	74.1	50.1	0.53	61.0	76.0	53.0	0.55	54.0	74.2	52.0	0.52	50.1	72.1	48.0	0.48	57.5	74.5	51.5	0.53	58.4	74.0	48.5	0.50
17	66.6	77.9	56.0	0.59	66.0	77.1	54.0	0.57	60.5	75.0	56.0	0.56	57.6	73.5	49.3	0.49	63.0	76.0	52.6	0.54	62.1	76.0	50.4	0.52
18	75.0	87.7	68.0	0.68	78.0	88.1	70.0	0.70	67.0	81.0	56.0	0.56	69.0	83.5	60.0	0.60	73.0	86.2	65.6	0.65	74.2	88.0	70.4	0.70
19	91.2	89.2	60.1	0.62	92.2	90.5	62.5	0.63	90.2	90.0	60.0	0.80	88.0	87.5	60.0	0.60	87.5	87.0	56.7	0.76	90.1	87.7	58.0	0.75
20	83.7	90.3	65.2	0.64	86.0	91.4	67.0	0.65	82.0	90.2	66.4	0.66	75.0	87.6	63.1	0.63	79.0	88.6	62.7	0.62	83.0	90.0	64.6	0.63
22	91.5	92.6	68.2	0.71	89.3	91.0	62.2	0.61	77.0	81.0	50.0	0.51	82.1	88.1	64.0	0.63	86.5	89.5	66.3	0.68	88.0	90.1	63.0	0.64
23	81.2	85.2	59.0	0.57	81.1	84.3	59.0	0.58	75.2	83.0	54.3	0.53	69.2	80.2	54.3	0.54	75.2	82.0	55.0	0.55	78.0	82.3	55.2	0.55
Mean	**79.7**	**83.6**	**62.0**	**0.61**	**79.5**	**83.4**	**61.5**	**0.61**	**73.0**	**81.0**	**58.0**	**0.59**	**70.4**	**80.5**	**57.7**	**0.57**	**74.7**	**82.0**	**59.0**	**0.61**	**76.5**	**82.4**	**58.9**	**0.60**

TABLE V
EVALUATED CLASSIFICATION PERFORMANCE PARAMETERS WITH FIVE-FOLD CROSS-VALIDATION USING DIFFERENT CLASSIFIERS FOR EOG

Sb	Ensemble boosted				Ensemble bagged				Ensemble subspace KNN				Fine tree				Medium tree				Coarse tree			
	Acc	Spe	Sen	F1	Acc	Spe	Sen	F1	Acc	Spe	Sen	F1	Acc	Spe	Sen	F1	Acc	Spe	Sen	F1	Acc	Spe	Sen	F1
1	79.0	88.5	66.2	0.67	80.0	88.6	67.7	0.69	77.5	88.2	69.0	0.69	71.5	85.0	62.8	0.63	76.8	87.8	69.1	0.69	77.3	88.0	69.2	0.70
2	92.4	89.0	78.5	0.83	93.0	88.0	75.1	0.79	83.0	77.6	58.6	0.61	89.1	86.7	71.3	0.70	89.0	86.1	69.1	0.70	90.0	89.0	73.4	0.73
3	83.8	78.0	58.3	0.61	84.2	80.0	62.0	0.64	79.2	79.6	63.0	0.62	78.1	79.8	62.8	0.61	82.7	79.5	61.7	0.64	85.2	80.1	62.1	0.66
4	71.0	82.0	60.2	0.62	69.0	80.4	57.0	0.59	60.0	75.6	50.0	0.50	61.5	76.7	51.1	0.51	66.2	80.0	57.6	0.58	67.0	80.0	54.3	0.55
5	63.0	79.8	62.0	0.63	60.0	78.2	59.1	0.60	52.7	75.1	51.7	0.52	57.4	77.5	57.3	0.57	60.1	78.5	60.0	0.60	64.4	81.0	64.5	0.65
6	75.2	85.3	64.0	0.62	75.0	85.7	64.1	0.63	63.3	80.7	56.6	0.56	64.3	81.7	59.3	0.59	73.0	85.0	63.6	0.63	74.0	85.1	64.6	0.64
7	75.2	86.6	74.8	0.76	76.5	87.1	75.6	0.64	69.0	83.0	68.0	0.69	68.4	82.7	67.2	0.68	71.0	84.0	69.0	0.70	74.0	86.0	73.1	0.74
9	87.1	74.3	64.4	0.62	87.7	75.0	65.0	0.63	81.0	75.6	64.1	0.64	79.0	75.5	65.5	0.64	81.1	73.0	61.0	0.61	83.0	74.6	63.1	0.64
10	87.7	84.4	62.5	0.62	87.2	85.1	64.0	0.65	82.2	85.1	62.1	0.60	79.8	82.1	58.1	0.59	81.7	83.4	58.0	0.59	84.0	82.6	58.4	0.59
11	74.6	74.0	56.4	0.59	73.0	73.0	55.0	0.58	67.0	74.2	56.0	0.56	67.5	75.1	60.0	0.58	67.5	72.0	50.5	0.52	72.1	71.0	50.0	0.51
14	88.0	93.2	66.5	0.60	88.1	93.5	68.0	0.68	84.0	92.0	69.2	0.69	82.8	92.0	69.5	0.69	85.5	93.0	68.3	0.69	87.2	93.2	69.1	0.70
16	66.3	79.0	60.1	0.61	63.7	77.4	59.0	0.60	55.7	75.3	54.7	0.55	57.2	75.6	55.6	0.56	60.0	75.2	54.0	0.54	64.3	77.5	58.0	0.58
17	65.0	76.0	59.0	0.61	66.3	76.5	59.0	0.63	59.5	73.7	59.4	0.59	60.1	74.8	56.4	0.56	59.5	72.7	53.6	0.55	62.6	74.5	54.0	0.56
18	72.0	84.2	62.4	0.63	71.2	83.6	61.0	0.62	69.4	83.2	60.0	0.60	61.6	78.9	52.0	0.52	67.9	82.7	60.0	0.60	67.8	82.1	59.0	0.59
19	92.0	90.0	61.5	0.62	90.6	88.6	59.0	0.76	89.8	88.8	63.2	0.64	86.1	85.6	55.0	0.69	87.0	87.0	57.0	0.58	89.2	87.2	57.2	0.60
20	83.6	90.3	65.0	0.63	83.2	90.1	64.5	0.63	75.4	87.3	63.0	0.63	75.4	87.7	64.4	0.64	79.5	89.1	66.0	0.66	81.3	89.7	65.4	0.65
22	88.6	91.3	65.1	0.65	88.6	90.0	65.1	0.68	84.7	90.1	66.0	0.65	84.3	89.2	67.0	0.66	84.6	88.7	63.0	0.64	85.1	89.0	63.1	0.64
23	83.1	86.2	61.0	0.59	82.0	85.0	60.0	0.60	75.7	84.3	59.0	0.60	73.1	82.6	55.4	0.55	78.1	85.4	61.3	0.61	77.2	83.0	54.0	0.53
Mean	**79.3**	**84.0**	**63.8**	**0.64**	**78.9**	**83.6**	**63.3**	**0.65**	**72.8**	**81.6**	**60.8**	**0.61**	**72.1**	**81.6**	**60.6**	**0.61**	**75.1**	**82.4**	**61.3**	**0.62**	**77.0**	**83.0**	**61.8**	**0.63**

MT) with different parametric settings, which is shown in Table III. In order to understand the computational complexity of proposed drowsiness recognition models, we have selected these classifiers, each characterized by a different level of layer complexity. Within this classification approach, the Ensemble-based classifier framework exhibits significant computational complexity, while the decision tree-based classifier framework is comparatively less computationally intensive.

Table IV shows the evaluated classification performance parameters with five-fold cross-validation using different classifiers for EEG signals. The EBT classifier outperformed all other classifiers with the highest average accuracy (79.7%) and F1 score (0.61). Additionally, it also exhibited the greatest average specificity (83.6%) and average sensitivity (62%) among all the classifiers. The FnT classifier had the lowest average accuracy (70.4%) and F1 score (0.57) among all classifiers. Subject 19 achieved the highest performance metrics with an accuracy of 92.2% and an F1 score of 0.62 when utilizing the EB classifier. Conversely, Subject 5 exhibited the least favourable results, recording an accuracy of 48% with the ESKNN classifier and an F1 score of 0.39 with the EBT classifier. Among the subjects, Subject 22 demonstrated exceptional specificity, attaining a value of 92.6% with the EBT classifier. On the other hand, Subject 11 displayed the lowest specificity, registering 68% with the EB classifier. In terms of sensitivity, Subject 7 stood out with the highest score, achieving 77.6% when employing the EBT classifier. Conversely, Subject 11 had the lowest sensitivity among all subjects, with a value of 40% when using the EB classifier.

Table V shows how well different classifiers can classify EOG signals into different classes. The EBT classifier has the highest average accuracy (79.3%), specificity (84%), and sensitivity (63.8%). The ESKNN classifier had the lowest average specificity (81.6%) and the lowest average accuracy (72.1%). Finally, the EB classifier had the highest average F1-score, 0.65, while the FnT classifier had the lowest, 0.61. Subject 2 did well, with a high accuracy of 93% when they used the EB classifier. But subject 5 did not do as well, we only got 52.7% accuracy with the ESKNN classifier. Subject 14 did exceptionally well in terms of specificity, getting 93.5% with the EBT classifier. However, subject 11 did not do so well in specificity, only getting 68% with the CT classifier. When it comes to sensitivity, subject 2 had the highest score, reaching 78.5% with the EBT classifier. On the flip side, subject 4 had the lowest sensitivity of all the subjects, with a score of 50% when using the ESKNN classifier. Subject 2 has achieved a high F1 score of 0.83 with the EBT classifier, and subject 4 has a low F1 score of 0.50 with the ESKNN classifier. From this table, we observed that EOG data classifier performance almost shows the same results compared with EEG data.

TABLE VI
EVALUATED CLASSIFICATION PERFORMANCE PARAMETERS WITH 5-FOLD CROSS-VALIDATION USING DIFFERENT CLASSIFIERS FOR A COMBINATION OF EEG AND EOG (CHANNEL FUSION MODEL)

Sb	Ensemble boosted				Ensemble bagged				Ensemble subspace KNN				Fine tree				Medium tree				Coarse tree			
	Acc	Spe	Sen	F1	Acc	Spe	Sen	F1	Acc	Spe	Sen	F1	Acc	Spe	Sen	F1	Acc	Spe	Sen	F1	Acc	Spe	Sen	F1
1	84.6	92.0	76.0	0.65	84.3	91.2	76.2	0.77	77.5	88.3	70.0	0.70	78.2	88.6	70.1	0.70	81.0	90.0	74.0	0.74	81.0	90.7	80.2	0.77
2	90.5	85.0	70.3	0.73	90.4	80.3	62.8	0.67	86.3	80.3	64.1	0.63	87.1	84.7	67.1	0.66	86.5	82.6	64.0	0.64	89.4	84.3	67.5	0.68
3	90.5	86.3	73.8	0.79	89.0	84.3	70.0	0.74	81.0	79.0	61.0	0.62	84.1	85.1	72.0	0.71	85.1	84.8	71.3	0.72	87.0	82.7	66.4	0.71
4	73.4	83.0	58.0	0.61	72.3	81.5	56.0	0.59	61.0	75.6	54.0	0.54	63.0	77.2	53.0	0.53	65.5	79.0	51.0	0.52	68.4	79.5	52.1	0.54
5	66.0	81.4	65.1	0.66	65.2	81.2	65.0	0.65	51.3	74.3	51.1	0.51	54.0	75.3	54.0	0.54	58.5	77.5	58.0	0.59	60.5	79.0	61.0	0.61
6	77.4	86.3	65.4	0.64	76.5	86.0	65.0	0.62	71.0	84.1	62.6	0.62	66.4	83.0	61.0	0.61	73.0	85.0	63.7	0.64	76.0	85.3	63.2	0.59
7	80.1	90.0	80.0	0.71	82.0	90.0	80.5	0.82	75.0	86.1	75.0	0.75	71.4	85.0	70.6	0.70	73.6	85.7	72.3	0.73	75.2	86.3	74.6	0.76
9	90.1	82.0	72.5	0.77	90.0	82.0	73.7	0.76	85.4	76.7	68.0	0.68	83.5	80.0	70.0	0.69	85.3	81.0	71.2	0.72	89.0	83.0	74.3	0.76
10	89.3	88.0	68.2	0.68	89.4	88.0	69.1	0.67	89.4	90.0	72.6	0.72	84.5	87.6	67.0	0.67	84.3	87.5	65.2	0.66	89.4	88.7	71.0	0.71
11	75.1	73.6	53.0	0.55	74.1	71.4	51.5	0.54	68.0	73.3	53.4	0.55	65.8	73.7	55.1	0.55	70.3	74.0	53.4	0.57	71.0	71.3	50.3	0.54
14	90.2	94.2	70.2	0.70	88.6	93.6	68.5	0.68	85.0	92.1	65.4	0.65	85.0	92.5	70.0	0.70	84.0	92.2	68.7	0.69	88.0	93.5	70.0	0.70
16	70.1	81.2	65.0	0.67	69.0	81.0	64.1	0.66	59.0	76.6	58.1	0.59	57.2	76.0	56.0	0.56	62.0	77.4	58.5	0.60	66.5	78.5	59.0	0.61
17	70.1	80.4	66.4	0.69	71.0	81.0	66.0	0.68	65.5	77.2	66.5	0.67	65.7	78.2	63.2	0.63	70.6	80.4	65.0	0.67	68.5	78.0	60.0	0.62
18	77.3	87.8	70.0	0.70	76.1	87.6	68.0	0.68	75.0	86.7	65.6	0.66	69.0	84.0	61.2	0.61	71.6	85.3	64.0	0.64	70.0	83.0	60.0	0.60
19	93.2	92.0	65.0	0.66	92.0	90.1	62.0	0.62	90.5	90.0	61.6	0.61	88.4	89.0	63.0	0.62	87.0	87.0	60.1	0.60	89.7	88.5	59.8	0.60
20	84.1	91.0	66.6	0.66	84.4	91.0	66.0	0.64	83.0	91.0	67.6	0.68	78.0	89.1	68.0	0.68	83.0	91.0	70.4	0.71	84.1	90.1	66.5	0.66
22	94.0	95.0	75.0	0.78	93.0	93.5	68.0	0.69	86.7	91.0	66.7	0.67	87.0	91.1	71.0	0.70	88.4	92.3	70.5	0.70	89.0	92.0	68.0	0.69
23	85.8	88.0	66.5	0.68	83.5	86.6	62.6	0.62	80.6	86.2	65.6	0.66	78.5	86.3	63.7	0.63	80.0	85.7	64.0	0.64	80.7	84.2	58.0	0.55
Mean	**82.3**	**86.5**	**68.2**	**0.69**	**81.7**	**85.6**	**66.4**	**0.67**	**76.2**	**83.3**	**63.8**	**0.64**	**74.6**	**83.7**	**64.2**	**0.64**	**77.2**	**84.4**	**64.7**	**0.65**	**79.1**	**84.4**	**64.5**	**0.65**

TABLE VII
EVALUATED CLASSIFICATION PERFORMANCE PARAMETERS WITH 5-FOLD CROSS-VALIDATION USING DIFFERENT CLASSIFIERS FOR FEATURE COMBINATION (FEATURE FUSION MODEL)

Sb	Ensemble boosted				Ensemble bagged				Ensemble subspace KNN				Fine tree				Medium tree				Coarse tree			
	Acc	Spe	Sen	F1	Acc	Spe	Sen	F1	Acc	Spe	Sen	F1	Acc	Spe	Sen	F1	Acc	Spe	Sen	F1	Acc	Spe	Sen	F1
1	82.6	90.6	74.1	0.75	84.0	91.5	74.8	0.76	79.0	89.0	71.1	0.71	78.4	88.9	70.0	0.70	80.0	89.5	71.6	0.72	80.0	89.0	65.1	0.65
2	89.0	81.3	61.0	0.65	92.5	87.7	74.0	0.77	86.7	80.0	61.0	0.63	88.2	87.0	70.0	0.68	89.4	86.0	70.7	0.70	91.0	90.7	77.6	0.75
3	90.0	85.3	72.0	0.77	88.0	82.1	65.8	0.70	82.1	79.0	60.5	0.62	82.2	81.6	65.1	0.66	83.0	81.0	64.7	0.66	87.0	82.3	66.1	0.71
4	72.1	82.2	57.0	0.59	69.0	79.5	49.6	0.50	59.5	75.1	48.1	0.48	61.1	77.6	49.4	0.48	68.4	80.5	50.5	0.51	67.8	80.0	50.0	0.50
5	63.3	80.0	63.0	0.64	63.7	80.5	63.4	0.64	53.5	75.2	53.1	0.53	55.5	76.5	55.6	0.55	56.0	76.2	55.0	0.56	60.0	78.0	58.0	0.59
6	76.4	86.0	65.1	0.63	75.0	85.2	63.5	0.62	70.4	83.7	62.7	0.62	64.0	82.0	59.6	0.59	71.0	84.0	61.7	0.61	73.5	84.6	64.0	0.63
7	80.2	89.2	79.0	0.80	80.1	89.0	78.6	0.80	72.1	84.5	71.2	0.72	70.0	84.0	69.3	0.69	73.0	85.3	72.5	0.73	72.5	84.7	71.6	0.73
9	91.1	84.0	77.5	0.79	89.3	81.1	72.2	0.75	83.5	78.0	70.4	0.70	84.5	82.0	73.5	0.73	84.7	80.6	70.6	0.72	89.1	82.0	73.0	0.75
10	89.1	87.6	69.0	0.69	88.2	86.6	66.0	0.65	88.1	89.5	71.0	0.70	84.0	87.1	65.3	0.65	84.6	87.5	65.2	0.65	87.2	87.6	67.4	0.66
11	73.7	73.0	53.4	0.56	74.7	73.0	52.5	0.55	67.5	74.5	57.0	0.57	62.7	70.0	50.1	0.50	69.0	72.5	51.4	0.53	70.0	70.0	49.0	0.49
14	90.0	94.1	70.7	0.71	87.6	93.3	69.0	0.69	84.3	92.0	66.0	0.65	82.7	92.0	67.7	0.67	84.3	92.2	68.2	0.68	87.0	93.1	70.0	0.70
16	67.5	80.0	62.5	0.64	65.5	79.0	60.6	0.62	61.6	78.6	61.4	0.61	60.0	77.5	59.2	0.59	63.0	77.7	59.0	0.60	62.5	77.0	56.3	0.59
17	67.5	78.7	63.0	0.65	69.0	79.2	62.0	0.65	66.2	78.2	67.2	0.67	59.5	75.1	53.6	0.53	65.2	77.6	60.5	0.61	63.3	78.6	60.7	0.60
18	78.4	89.0	72.6	0.72	77.0	88.0	70.0	0.70	74.7	86.0	65.7	0.66	72.0	85.2	64.5	0.64	71.0	85.4	64.5	0.64	72.4	87.1	68.7	0.67
19	91.2	88.3	58.5	0.63	92.5	90.6	61.2	0.60	90.4	90.0	60.2	0.60	85.3	87.7	60.1	0.59	85.5	85.1	55.5	0.56	89.1	88.0	58.5	0.59
20	85.3	91.5	67.0	0.66	85.3	91.3	67.0	0.66	83.0	91.0	67.6	0.68	76.0	88.2	64.0	0.64	79.1	89.3	66.0	0.66	83.7	90.5	65.5	0.64
22	94.0	95.0	75.5	0.79	91.4	92.0	64.3	0.64	87.7	91.6	69.0	0.69	86.0	90.4	69.3	0.69	85.1	90.0	65.1	0.65	88.1	90.3	67.8	0.70
23	83.0	86.3	61.4	0.60	82.6	85.7	61.5	0.62	78.5	84.0	56.0	0.56	73.2	83.5	59.6	0.60	76.1	82.5	54.7	0.55	77.3	83.6	56.6	0.56
Mean	**81.3**	**85.7**	**66.8**	**0.68**	**80.9**	**85.3**	**65.3**	**0.66**	**76.1**	**83.3**	**63.3**	**0.63**	**73.6**	**83.1**	**62.5**	**0.62**	**76.0**	**83.5**	**62.6**	**0.63**	**77.8**	**84.3**	**63.6**	**0.64**

In our study, we have used two distinct modalities combined techniques. Firstly considering multivariate channel data, we employed both EEG and EOG raw data. After data decomposition, we extracted the features of each mode and provided them as input to the classifier. Table VI shows how well different classifiers can classify the combination of EEG and EOG channels into different classes. The FnT classifier has the lowest average accuracy (74.6%), while the EBT classifier has the best (82.3%). Ensemble Boosted has the highest average specificity (86.5%), while ESKNN has the lowest (83.3%). The Ensemble Subspace KNN classifier has the lowest average sensitivity (63.8%), while the EBT classifier has the greatest (68.2%). The FnT classifier has the lowest average F1-score (0.64), and the Ensemble Boosted classifier has the highest (0.69). Each classifier's performance across subjects is also included in the table. Subject 22 has the greatest accuracy for all classifiers except Ensemble Subspace KNN (86.7%), whereas subject 5 has the lowest. Subject 22 has the highest classifier specificity (over 90%), whereas subject 11 has the lowest. Subject 7 has the highest EB classifier sensitivity (80.5%), and subject 4 has the lowest MT classifier sensitivity (51%). Subject 7 also has the greatest EB F1-score (0.82), whereas subject 5 has the lowest ESKNN F1-score (0.51).

Secondly, the retrieved features from the EEG and EOG are simply concatenated into a bigger feature matrix, and this larger feature matrix is provided as input to the classifier model. Table VII represents the performance with features combination of EEG and EOG channels. From this table, we observed that he EBT classifier excels in various aspects, boasting the highest average accuracy at 81.3%, leading in average specificity with 85.7%, and outperforming others with an average sensitivity of 66.8%. Additionally, it achieves the highest average F1-score at 0.68, while the FnT classifier falls behind with the lowest average accuracy of 73.6%, specificity of 83.1%, sensitivity of 62.5%, and an average F1-score of 0.62. From Table VI-VII, it is observed that, out of two modalities, the features combined method shows slightly inferior results in terms of performance parameters. Subject 22 exhibits the highest accuracy (94%) at the EBT classifier, while subject 5 demonstrates the lowest accuracy (53.5%) using the ESKNN classifier. Subject 14 showcases the highest specificity (94.1%) at the EBT classifier, whereas subject 11 displays the lowest specificity (70%) at CT classifiers. In addition, subject 7 boasts the highest sensitivity (79%) at EBT classifiers, whereas subject 4 presents the lowest sensitivity (48.1%) at ESKNN classifier. Subject 7 also records the highest F1-score 0.80 at

TABLE VIII
PERFORMANCE COMPARISON WITH THE STATE OF THE ART METHODS FOR DROWSINESS DETECTION

Reference and year	Classifier	Number of classes	Physiological signal	Accuracy	Dataset used
Hasan et al. [29] (2022)	ANN	2	EEG and EOG	75.0%	[29]
	SVM			79.0%	
Barua et al. [30] (2019)	KNN	3	EEG and EOG	78.0%	VTI [31]
	RF			77.0%	
Zheng et al. [6] (2017)	SVR		EEG	75.0%	
	SVR	3	EOG	79.0%	SEED-VIG
	SVM			72.0%	
Hidalgo et al. [32](2022)	KNN	3	EEG	71.0%	SEED-VIG
	RF			74.0%	
	SVM			78.6%	
Gwak et al. [33] (2018)	KNN	2	ECG and EEG	75.3%	[33]
	RF			81.4%	
	EBT			82.3%	
Proposed framework-1	EB	3	EEG and EOG channel fusion	81.7%	SEED-VIG
	CT			79.1%	
	EBT			81.3%	
Proposed framework-2	EB	3	EEG and EOG feature fusion	80.9%	SEED-VIG
	CT			77.8%	

EB classifiers, while subject 11 records the lowest F1-score 0.48 at FnT classifiers.

Table VIII presents a comprehensive performance comparison of various methods used for drowsiness detection based on physiological signals. These methods have been applied to different datasets and utilize different classification techniques to achieve accurate predictions regarding drowsiness levels. The table primarily focuses on accuracy as a performance metric, highlighting the effectiveness of each method in correctly classifying drowsiness across multiple classes. Hasan et al [29] introduced a drowsiness detection approach using ANN and SVM classifiers. Their method employs EEG and EOG signals, achieving accuracies of 75.0% and 79.0% respectively. Barua et al [30] utilized k-nearest neighbour (KNN) and random forest (RF) classifiers on EEG and EOG signals, achieving accuracies of 78.0% and 77.0% respectively on the VTI dataset. Zheng et al [6] employed Support Vector Regression (SVR) for EEG and EOG signals with a three-class approach, achieving 75.0% and 79.0% accuracy, respectively on the SEED-VIG dataset. They also employed SVM achieving 72.0% accuracy. Hidalgo et al [32] used KNN, RF, and SVM classifiers on EEG signals achieving accuracies of 71.0%, 74.0%, and 78.6% respectively on the SEED-VIG dataset. Gwak et al [33] integrated ECG and EEG signals using KNN, RF, and SVM classifiers, obtaining accuracies of 75.3%, 81.4%, and 78.6% respectively. Both models utilize EEG and EOG multi-channel signals and incorporate various classifiers and feature combinations. In proposed framework-1, the EBT classifier and CT classifier are employed, achieving accuracy rates of 82.3% and 79.1%, respectively. Additionally, the EB classifier reaches an accuracy of 81.7%. In proposed framework-2, an accuracy of 81.3% is attained using the EBT classifier. The CT classifier is combined with extracted features, resulting in a slightly lower accuracy of 77.8%.

V. CONCLUSION

In this research, we introduce a novel multivariate empirical Fourier decomposition method that leverages hybrid signal modalities (EEG and EOG) to classify different drowsiness states i.e. alert, tired, and drowsy. The proposed MEFD is designed specifically for multivariate multichannel signal analysis and decomposes into channel-aligned modes, employing adaptive frequency scales to alleviate mode alignment issues in multi-channel data. To evaluate our approach, we have conducted extensive experiments employing six machine learning classifiers, including EBT, EB, ESKNN, FnT, MT, and CT, while assessing performance metrics such as accuracy, specificity, sensitivity, and the F1 score. Among these classifiers, the EBT-based classification framework has shown the best performance, achieving the highest accuracy across different channel fusion schemes. Thus, the proposed method can be demonstrated as a more realistic and reliable approach in recognizing drowsiness states. In the future, this framework for analyzing multivariate data can be extended to include a larger number of channels and a deeper classification framework, incorporating diverse cross-modal signals, for the development of a feasible clinical model.

REFERENCES

[1] A. Chowdhury, R. Shankaran, M. Kavakli, and M. M. Haque, "Sensor applications and physiological features in drivers' drowsiness detection: A review," *IEEE Sensors Journal*, vol. 18, no. 8, pp. 3055–3067, 2018.
[2] S. K. Lal and A. Craig, "A critical review of the psychophysiology of driver fatigue," *Biological Psychology*, vol. 55, no. 3, pp. 173–194, 2001.
[3] A. K. Das, P. Kumar, S. Halder, A. Banerjee, and D. Tibarewala, "A laboratory based experimental evaluation of ocular parameters as fatigue and drowsiness measures," *Procedia Computer Science*, vol. 167, pp. 2051–2059, 2020.
[4] Y. Sun, X. Yu, J. Berilla, Z. Liu, and G. Wu, "An in-vehicle physiological signal monitoring system for driver fatigue detection," in *3rd International Conference on Road Safety and Simulation Purdue University Transportation Research Board*, 2011.
[5] I. Stancin, M. Cifrek, and A. Jovic, "A review of EEG signal features and their application in driver drowsiness detection systems," *Sensors*, vol. 21, no. 11, p. 3786, 2021.
[6] W.-L. Zheng and B.-L. Lu, "A multimodal approach to estimating vigilance using EEG and forehead EOG," *Journal of Neural Engineering*, vol. 14, no. 2, p. 026017, 2017.
[7] R.-C. Wu, C.-T. Lin, S.-F. Liang, T.-Y. Huang, and T.-P. Jung, "EEG-based fuzzy neural network estimator for driving performance," in *2004 IEEE International Conference on Systems, Man and Cybernetics (IEEE Cat. No. 04CH37583)*, vol. 4, pp. 4034–4040, IEEE, 2004.
[8] C.-T. Lin, R.-C. Wu, S.-F. Liang, W.-H. Chao, Y.-J. Chen, and T.-P. Jung, "EEG-based drowsiness estimation for safety driving using independent component analysis," *IEEE Transactions on Circuits and Systems I: Regular Papers*, vol. 52, no. 12, pp. 2726–2738, 2005.

[9] M. B. Dkhil, A. Wali, and A. M. Alimi, "Drowsy driver detection by EEG analysis using fast fourier transform," in *2015 15th International Conference on Intelligent Systems Design and Applications (ISDA)*, pp. 313–318, IEEE, 2015.
[10] I. Belakhdar, W. Kaaniche, R. Djmel, and B. Ouni, "A comparison between ANN and SVM classifier for drowsiness detection based on single EEG channel," in *2016 2nd International Conference on Advanced Technologies for Signal and Image Processing (ATSIP)*, pp. 443–446, IEEE, 2016.
[11] A. Picot, S. Charbonnier, and A. Caplier, "On-line detection of drowsiness using brain and visual information," *IEEE Transactions on Systems, man, and cybernetics-part A: systems and humans*, vol. 42, no. 3, pp. 764–775, 2011.
[12] L.-l. Chen, Y. Zhao, J. Zhang, and J.-z. Zou, "Automatic detection of alertness/drowsiness from physiological signals using wavelet-based nonlinear features and machine learning," *Expert Systems with Applications*, vol. 42, no. 21, pp. 7344–7355, 2015.
[13] A. Zhang and Y. Chen, "EEG feature extraction and analysis under drowsy state based on energy and sample entropy," in *2012 5th International Conference on BioMedical Engineering and Informatics*, pp. 501–505, IEEE, 2012.
[14] T. d. Silveira, A. d. J. Kozakevicius, and C. R. Rodrigues, "Drowsiness detection for single channel EEG by DWT best m-term approximation," *Research on Biomedical Engineering*, vol. 31, pp. 107–115, 2015.
[15] T. L. da Silveira, A. J. Kozakevicius, and C. R. Rodrigues, "Automated drowsiness detection through wavelet packet analysis of a single EEG channel," *Expert Systems with Applications*, vol. 55, pp. 559–565, 2016.
[16] A. G. Correa, L. Orosco, and E. Laciar, "Automatic detection of drowsiness in EEG records based on multimodal analysis," *Medical Engineering & Physics*, vol. 36, no. 2, pp. 244–249, 2014.
[17] R. Wang, Y. Wang, and C. Luo, "EEG-based real-time drowsiness detection using hilbert-huang transform," in *2015 7th International Conference on Intelligent Human-Machine Systems and Cybernetics*, vol. 1, pp. 195–198, IEEE, 2015.
[18] R. B. Pachori, *Time-frequency analysis techniques and their applications*. CRC Press, 2023.
[19] Y. Ed-Doughmi and N. Idrissi, "Driver fatigue detection using recurrent neural networks," in *Proceedings of the 2nd International Conference on Networking, Information Systems & Security*, pp. 1–6, 2019.
[20] J.-H. Jeong, B.-W. Yu, D.-H. Lee, and S.-W. Lee, "Classification of drowsiness levels based on a deep spatio-temporal convolutional bidirectional lstm network using electroencephalography signals," *Brain Sciences*, vol. 9, no. 12, p. 348, 2019.
[21] H. Alaskar, "Convolutional neural network application in biomedical signals," *J Comput Sci Inform Tech*, vol. 6, no. 2, pp. 45–59, 2018.
[22] S. Rajwal and S. Aggarwal, "Convolutional neural network-based eeg signal analysis: A systematic review," *Archives of Computational Methods in Engineering*, pp. 1–31, 2023.
[23] W. Zhou, Z. Feng, Y. Xu, X. Wang, and H. Lv, "Empirical fourier decomposition: An accurate signal decomposition method for nonlinear and non-stationary time series analysis," *Mechanical Systems and Signal Processing*, vol. 163, p. 108155, 2022.
[24] A. Bhattacharyya and R. B. Pachori, "A multivariate approach for patient-specific EEG seizure detection using empirical wavelet transform," *IEEE Transactions on Biomedical Engineering*, vol. 64, no. 9, pp. 2003–2015, 2017.
[25] J. Gilles, "Empirical wavelet transform," *IEEE Transactions on Signal Processing*, vol. 61, no. 16, pp. 3999–4010, 2013.
[26] S. V. Bhalerao and R. B. Pachori, "Sparse spectrum based swarm decomposition for robust nonstationary signal analysis with application to sleep apnea detection from eeg," *Biomedical Signal Processing and Control*, vol. 77, p. 103792, 2022.
[27] K. Biju, M. Jibukumar, and C. Rajasekharan, "EEG analysis using a wavelet packet transforms mean energy and mean teager energy with an artificial neuro-fuzzy system," *Exergy for A Better Environment and Improved Sustainability 2: Applications*, pp. 627–635, 2018.
[28] Z.-H. Zhou, *Machine learning*. Springer Nature, 2021.
[29] M. M. Hasan, C. N. Watling, and G. S. Larue, "Physiological signal-based drowsiness detection using machine learning: Singular and hybrid signal approaches," *Journal of Safety Research*, vol. 80, pp. 215–225, 2022.
[30] S. Barua, M. U. Ahmed, C. Ahlström, and S. Begum, "Automatic driver sleepiness detection using EEG, EOG and contextual information," *Expert Systems with Applications*, vol. 115, pp. 121–135, 2019.
[31] C. Fors, C. Ahlstrom, and A. Anund, "A comparison of driver sleepiness in the simulator and on the real road," *Journal of Transportation Safety & Security*, vol. 10, no. 1-2, pp. 72–87, 2018.
[32] J. M. H. Rogel, E. T. M. Beltrán, M. Q. Pérez, S. L. Bernal, G. M. Pérez, and A. H. Celdrán, "Studying drowsiness detection performance while driving through scalable machine learning models using electroencephalography," *arXiv preprint arXiv:2209.04048*, 2022.
[33] J. Gwak, M. Shino, and A. Hirao, "Early detection of driver drowsiness utilizing machine learning based on physiological signals, behavioral measures, and driving performance," in *2018 21st International Conference on Intelligent Transportation Systems (ITSC)*, pp. 1794–1800, IEEE, 2018.
[34] R. Sharma and R. B. Pachori, "Classification of epileptic seizures in EEG signals based on phase space representation of intrinsic mode functions," *Expert Systems with Applications*, vol. 42, no. 3, pp. 1106–1117, 2015.
[35] A. Bansal and A. Singhrova, "Performance analysis of supervised machine learning algorithms for diabetes and breast cancer dataset," in *2021 International Conference on Artificial Intelligence and Smart Systems (ICAIS)*, pp. 137–143, IEEE, 2021.

Ashok Mahato received the M.Tech. degree in Electronics Engineering from the GUIST, Guwahati, India, in 2012. At present, he is a research scholar in the Department of Electrical Engineering at IIT Indore, Indore, India. His research interests include biomedical signal processing and brain computer interfacing.

Ram Bilas Pachori (Senior Member, IEEE) received the Ph.D. degree from IIT Kanpur, Kanpur, India, in 2008. He is currently a Professor at the Department of Electrical Engineering, IIT Indore, Indore, India. His research interests include signal and image processing, biomedical signal processing, nonstationary signal processing, speech signal processing, brain–computer interfacing, and machine learning.